Sensors and Actuators B 173 (2012) 239–243

Contents lists available at SciVerse ScienceDirect

Sensors and Actuators B: Chemical

journal homepage: www.elsevier.com/locate/snb

Sonoelectrochemical synthesized RGO–PbTe composite for novel electrochemical biosensor

Jian-Jun Shi[a,b], Wei Hu[a,b], Dan Zhao[b], Ting-Ting He[a], Jun-Jie Zhu[b,*]

[a] School of Chemical Engineering, Anhui University of Science and Technology, Huainan 232001, China
[b] State Key Laboratory of Analytical Chemistry for Life Science, School of Chemistry and Chemical Engineering, Nanjing University, Nanjing 210093, China

ARTICLE INFO

Article history:
Received 10 February 2012
Received in revised form 28 June 2012
Accepted 30 June 2012
Available online 10 July 2012

Keywords:
PbTe
Graphene
Nanocomposite
Pulse sonoelectrochemistry
Biosensor
Hydrogen peroxide

ABSTRACT

Reduced graphene oxide–lead tellurium (RGO–PbTe) composites were fabricated via sonoelectrochemical technique. The crystalline structure, composition and morphology of the products were characterized by X-ray powder diffraction (XRD), energy dispersive X-ray spectrometer (EDS), transmission electron microscopy (TEM), respectively. The results showed that the PbTe nanoparticles (NPs) were uniformly decorated on the RGO sheets. The formation mechanism of RGO–PbTe nanocomposite was proposed. Ultrasonic played an important role in the formation of PbTe NPs. The composites were further used as supports for immobilization of hemoglobin (Hb) to fabricate a novel electrochemical biosensor, which had good thermal stability, conductivity and biocompatibility and enhanced direct electron transfer. This biosensor showed excellent electrocatalytic activity towards H_2O_2 with a linear range from 0.5 to 30 μM and low detection limit as 0.13 μM.

1. Introduction

The direct electrochemistry of redox proteins has received considerable attention in recent years. The main objective in modern bioelectrochemistry is to facilitate direct electron transfer between the redox centers of enzymes and electrode surface. Nanomaterials have been successfully used to fabricate the third-generation electrochemical biosensors [1]. Among these, graphene has attracted tremendous interest due to its distinctive properties, such as large surface area and excellent conductivity [2,3]. Recent studies have demonstrated that graphene-based electrochemical biosensors involving catalase [4], cytochrome C [5,6], glucose oxidase [7,8], HRP [9,10], Hb [11] and so on.

Some methods have been developed to incorporate metal or metal oxide nanoparticles onto the graphene sheets, such as chemical reduction [12], electrostatic assembly [13], intercalation [14], chemical vapor deposition methods [15], sol–gel methods [16], and so on. Recently, we have also fabricated Pd–graphene [17] and PdPt–graphene [18] nanocomposites via sonoelectrochemical method. These nanoparticles not only prevent the aggregation of graphene sheets but also combine with the special two-dimensional graphene, giving rise to some unique electronic, optical and catalytical properties. On the other hand, graphene has been proven to be compatible in the construction of biosensors due to their good conductivity, high stability and loading of biomolecules [19].

Lead tellurium semiconductor nanocrystals have unique optical, electrical and chemical properties [20,21], and can be applied in solar cells [22,23], thermoelectric devices [24] and bio-image [25]. However, it is difficult to homogenously disperse nanostructures into other component matrix. Recently, PbTe–polyaniline core–shell nanocomposites [26] and PbTe-modified poly (3,4-ethylenedioxythiophene) (PEDOT) nanotubes [27] were prepared by in situ interfacial polymerization, exhibiting extremely large Seebeck coefficient values and enhanced thermoelectric properties. Thin lead chalcogenide film possesses good thermoelectric properties which were obtained by spin-coating procedure using a polymer/precursor mixture [28]. Moreover, carbon materials, such as graphene, also served as another kind of important components for the fabrication of nanocomposites [29].

Herein, RGO–PbTe nanocomposite was synthesized by sonoelectrochemical technique for the immobilization of Hb, and further integrated the RGO–PbTe–Hb bioconjugate to fabricate a biosensor for the determination of H_2O_2. The morphology, composition and structure of the composite were also well investigated, and the electrochemical behavior of the RGO–PbTe–Hb bioconjugate was discussed.

* Corresponding author. Tel.: +86 25 8359 7204; fax: +86 25 8359 7204.
E-mail address: jjzhu@nju.edu.cn (J.-J. Zhu).

0925-4005/$ – see front matter © 2012 Elsevier B.V. All rights reserved.
http://dx.doi.org/10.1016/j.snb.2012.06.091

2. Experimental

2.1. Reagents and apparatus

Bovine hemoglobin (Hb, MW. 64500), Nafion 117 (5%, w/v, in alcoholic solution) and Polyvinylpyrrolidone (PVP, K-30, M_w 40000) were purchased from Sigma–Aldrich. Graphite powder (99.95%, 325 mesh), lead nitrate ($Pb(NO_3)_2$), tellurium oxide (TeO_2), and nitrilotriacetic acid (NTA) were purchased from Chinese Shanghai Regent Co. Hydrazine hydrate, concentrated H_2SO_4, sodium hydroxide (NaOH), phosphorus oxide (P_2O_5) and hydrogen peroxide (H_2O_2) were obtained from Nanjing Chemical Reagents Factory (Nanjing, China). All reagents were analytical grade and directly used without further purification. All solutions were prepared with Millipore water. Phosphate buffer solution (PBS, pH 7.0, 0.1 mol L^{-1}) was used in all electrochemical studies unless otherwise stated.

A sonoelectrochemical device described previously [30–33] was employed to synthesize RGO–PbTe nanocomposite. In brief, a titanium horn (VC-750, 20 kHz, Sonics & Materials) acted both as the cathode and the ultrasound emitter with an effective area of 1.23 cm^2 at the bottom. A platinum sheet (1.0 cm × 1.0 cm) was used as counter electrode. Electrochemical measurements were performed using a CHI 660D electrochemical workstation. Cyclic voltammograms (CVs) and amperometric current–time curve (i–t) were obtained in a conventional three-electrode cell. A modified GC electrode was used as the working electrode, a Pt sheet as the counter electrode, and saturated calomel electrode (SCE) as the reference electrode. The electrolyte solution was deoxygenated with nitrogen and kept under nitrogen atmosphere during electrochemical experiments.

The phase composition of samples was determined by X-ray powder diffraction (XRD) performed on a Shimadzu XD-3A diffractometer with Cu Kα radiation (λ = 0.15418 nm). The morphology and composition were measured by transmission electron microscopy (TEM) on JEOL-2100 microscope equipped with an energy dispersive X-ray spectrometer (EDS) at 200 kV accelerating voltage. The UV–visible (UV–vis) absorption spectra were obtained on a photospectrometer (UV-3600, Shimadzu Co.).

2.2. Synthesis of RGO–PbTe nanocomposite

Firstly, graphite oxide (GO) was synthesized from natural graphite powder by modified Hummers method [34]. Then, 0.1 g PVP was added into 100 mL of 0.5 g L^{-1} GO solution and stirred for 30 min. The resulting dispersion was mixed with 0.5 mL 80% hydrazine hydrate and the reduction reaction was performed at 90 °C for 24 h under constant stirring. Successively, the black homogeneous reduced graphene oxide (RGO) aqueous dispersion (0.5 g L^{-1}) was purified by dialysis with a semipermeable membrane (M_w = 8000 Da) against deionized water for 36 h to remove the residual hydrazine. RGO–PbTe nanocomposite was prepared via sonoelectrochemical route as previously reported [35]. In a typical synthesis, 0.3 mL of NTA solution (0.2 mol L^{-1}), 6 mL of Na_2TeO_3 solution (0.005 mol L^{-1}), obtained by reaction of TeO_2 powder and NaOH, 0.1 g PVP and 0.5 mL of RGO solution (0.5 g L^{-1}) were added into 50 mL of $Pb(NO_3)_2$ solution (0.2 mol L^{-1}) in sequence under stirring. Then, the pH was adjusted to 8.5 with NaOH solution (0.1 mol L^{-1}). The RGO–PbTe composite was produced in a sonoreactor with a current pulse (20 mA, 0.5 s) immediately following a ultrasonic pulse (25 W, 0.3 s) and 0.2 s of silence. Finally, products were obtained after 1800 cycles of above pulse-repetition, followed by centrifugation (9000 rpm, 10 min), washing and dispersion in deionized water for several times.

2.3. Preparation of RGO–PbTe–Hb bioconjugates modified electrodes

For the fabrication of RGO–PbTe–Hb bioconjugates, 10 mg mL^{-1} of RGO–PbTe composite was dispersed in 200 μL of PBS (pH 7.0) containing 1 mg of Hb and shaken at room temperature overnight, followed by centrifugation and washing. The GCE with 3 mm in diameter was polished with 1.0, 0.3 and 0.05 μm α-alumina powder, and sonicated in ethanol and water successively. The obtained RGO–PbTe–Hb bioconjugates were re-suspended in 0.5 mL of water, and 10 μL of this suspension was dropped onto the electrode and dried in a silica gel desiccator. After 120 min, 10 μL of 0.5% (w/v) Nafion ethanol solution was dropped on the electrode surface and left at ambient conditions to evaporate the ethanol. Finally, the electrode was left to dry at 4 °C overnight. The RGO, RGO–PbTe and RGO–Hb modified electrodes were prepared in the same way except that RGO, RGO–PbTe or RGO–Hb was used instead of the bioconjugates. The modified electrode was stored under the same conditions when not used.

3. Results and discussion

3.1. Characterization of RGO–PbTe composite

Fig. 1A is the TEM image of the RGO–PbTe composite. The PbTe nanoparticles with the size of 10–20 nm are well separated and uniformly distributed on the graphene sheets, which indicates that they are firmly attached to graphene sheets. For comparison, PbTe was synthesized by the same method in the absence of graphene. Obvious agglomeration of PbTe nanoparticles can be observed in Fig. 1B. It indicated that PbTe nanoparticles could be effectively synthesized by sonoelectrochemical method, and RGO sheets may be responsible for dispersion of the nanoparticles under sonication. The presence of Pb and Te in the RGO–PbTe composites was also confirmed by EDS analysis as shown in Fig. 1C. The positions of energy peaks assigned to Pb and Te are consistent with that of PbTe. The EDS of PbTe and RGO were supplemented in Fig. S1. The peak assigned to C and Cu in the EDS analysis could be attributed to the mesh used for the TEM measurement. The result indicates that PbTe has been successfully deposited on the graphene sheets. XRD patterns of the pure RGO (curve a), PbTe (curve b) and RGO–PbTe (curve c) are given in Fig. 1D. The peak at $2\theta = 27.5°$ of RGO–PbTe indicates that PbTe is crystalline state.

3.2. Spectroscopic analysis and electrochemical impedance spectroscopy (EIS)

UV–vis spectroscopy is sensitive for the characteristic of proteins and the Soret absorption is at ca. 410 nm. Fig. 2A shows the UV–vis spectra of Hb, RGO–PbTe, RGO–PbTe–Hb, respectively. A characteristic Soret absorption band of RGO–PbTe–Hb was observed at ca.406 nm in PBS (curve b), the same as that of native state of Hb (curve a), while no absorption of RGO–PbTe was observed (curve c). This result suggests that Hb entrapped in RGO–PbTe composite kept its secondary structure and retains its biological activity.

Electrochemical impedance spectroscopy (EIS) was applied to monitoring whole procedure in the fabrication of modified electrode. Fig. 2B exhibits the impedance spectroscopy of different modified electrodes in the presence of equimolar $Fe(CN)_6^{3-/4-}$. The semicircle diameter in the impedance spectrum equals the electron-transfer resistance, R_{et}. This resistance controls the electron-transfer kinetics of the redox probe at the electrode interface. As observed in the curve (a) of Fig. 2B, the diameter of Nyquist circle shows the relatively facile charge transfer at bare electrode.

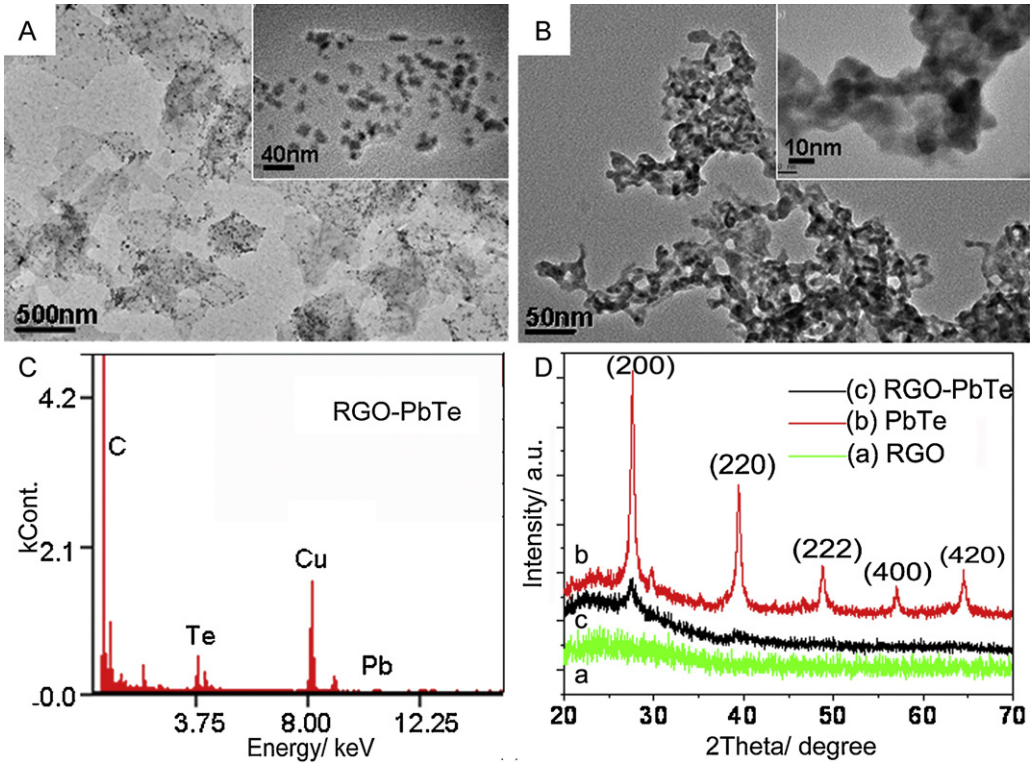

Fig. 1. TEM images of RGO–PbTe (A) and PbTe (B), EDS of the RGO–PbTe (C), and the XRD patterns (D) of the (a) RGO, (b) PbTe, and (c) RGO–PbTe.

After RGO–PbTe was coated on the electrode, a substantial decrease in the diameter of the semicircle was observed (curve c). Compared to RGO (curve b), RGO–PbTe exhibited a better electron-transfer property between the EIS probe and the electrode. When Hb was incorporated into RGO–PbTe nanocomposite film, the increased R_{et} was found (see curve d), which indicated that Hb was successfully immobilized on the composite film.

3.3. Direct electrochemistry of Hb–PbTe–RGO bioconjugates

The electrochemical behavior of the RGO–PbTe–Hb modified electrode was studied in 0.1 M PBS (pH 7.0) at 100 mV s^{-1}. Fig. 3 shows the cyclic voltammograms obtained from different modified electrodes. No any current peaks can be observed at the RGO modified electrode (curve a), indicating the nonelectroactive property in the surveyed potential window. After combining with Hb (curve b), a pair of small but stable and well-defined redox peaks appears, showing the electron transfer between Hb and the underlying electrode. The anodic and cathodic peak potentials are located

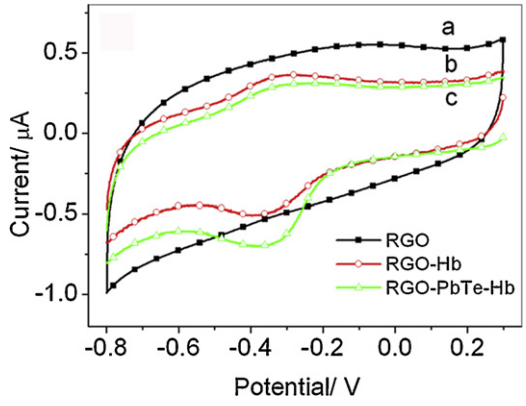

Fig. 3. Cyclic voltammograms of (a) RGO/GCE, (b) RGO–Hb/GCE, and (c) RGO–PbTe–Hb/GCE at a scan rate of 100 mV s^{-1}.

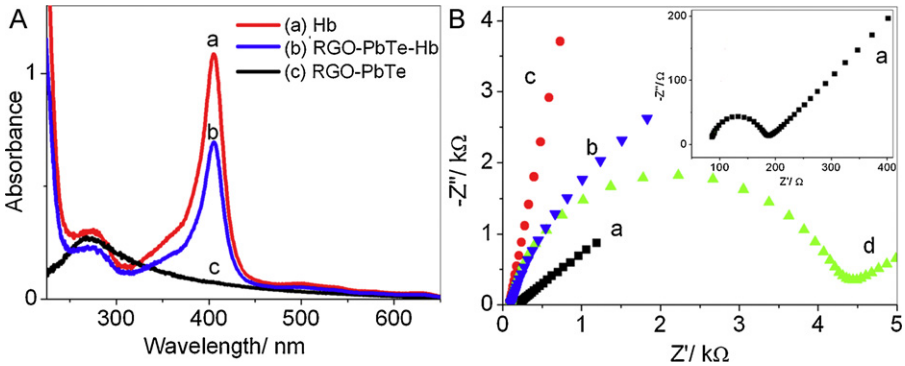

Fig. 2. (A) UV–vis spectra of (a) Hb, (b) RGO–PbTe–Hb, and (c) RGO–PbTe in 0.1 M pH 7.0 PBS. (B) Nyquist plots of modified GCE recorded in solution containing 0.1 M KCl and 10 mM $Fe(CN)_6^{3-}/Fe(CN)_6^{4-}$: (a) bare GCE, (b) RGO/GCE, (c) RGO–PbTe/GCE, and (d) RGO–PbTe–Hb/GCE.

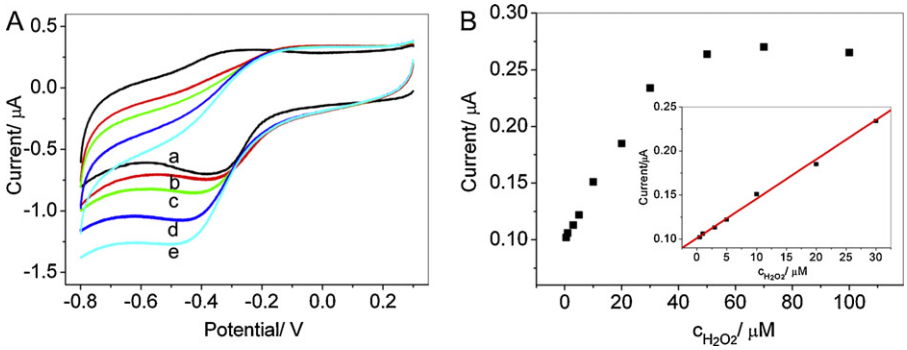

Fig. 4. (A) Cyclic voltammograms of the RGO–PbTe–Hb at a scan rate of 100 mV s^{-1} in 0.1 M pH 7.0 PBS solutions with (a) 0, (b) 5.0, (c) 10.0, (d) 30.0, (e) 50.0 μM H_2O_2. (B) Plots of the electrocatalytic current (i) vs. H_2O_2 concentration. Inset: linear plots of i vs. H_2O_2 concentration.

at −0.28 and −0.37 V (vs. SCE) respectively. In Fig. 3 (curve c), the electrode modified with the RGO–PbTe–Hb composite shows a pair of enhanced redox peaks, which indicates that Hb is successfully immobilized on the RGO–PbTe composite, and the heme groups in Hb molecules still retain their structure and activity. This may be ascribed to synergistic effects of the good conductivity, the huge surface area and the catalytic effect of RGO–PbTe. The RGO–PbTe served as a suitable supporting component of biosensor, which promoted the electron transfer.

The dependence of the peak currents (i_p) on the scan rate was studied. As shown in Fig. S2, the cathodic and anodic peak currents increase linearly with the scan rate range from 10 to 250 mV s^{-1}. Thus, the Hb adsorbed on the surface undergoes a surface controlled electron transfer. According to Faraday's law ($Q = nFA\Gamma$), where Q is the total amount of charge, n is the number of electron transferred, F is the Faraday's constant, and A is the electron area, the average Γ values of electroactive Hb can be estimated to be 5.41×10^{-11} mol cm^{-2}, which is larger than the theoretical monolayer coverage of Hb (1.89×10^{-11} mol cm^{-2}) [36]. This indicates that a multilayer of proteins participated in the electron transfer process in the composite.

3.4. The determination of hydrogen peroxide

Fig. 4A depicts the cyclic voltammograms obtained at a GCE modified with RGO–PbTe–Hb in PBS (pH 7.0) containing varied concentrations of H_2O_2. The reduction peak at approximately −0.35 V is greatly enhanced, while the anodic peak decreases, suggesting an electrocatalytic reduction of H_2O_2 occurred. Moreover, the reduction current increases dramatically with the increasing concentration of H_2O_2, while oxidation current becomes gradual disappearance. The calibration curve in Fig. 4B shows that the reduction peak current increases linearly with the concentration of H_2O_2 in the range from 0.5 to 30 μM. The linear regression equation is $y = 0.0045x + 0.1011$ μA, with a correlation coefficient of 0.9986. The sensitivity of the biosensor is 0.1 μA μM^{-1}, From the slope of 0.0045 μA μM^{-1}, the detection limit is estimated to be 0.13 μM from 3 times the standard deviation of the blank [37], which is much lower than other graphene-based biosensor for H_2O_2 [4,9].

When the concentration of H_2O_2 is higher than 50 μM, a CV response plateau is observed, showing a typical Michaelis–Menten kinetic mechanism. The apparent Michaelis–Menten constant (K_M^{app}) is calculated by Lineweaver–Burk equation $1/I_{ss} = 1/I_{max} + K_M^{app}/I_{max}c$ to evaluate the catalytic activity of intercalated protein and compare this sensor with others [38]. Here I_{ss} is the steady-state current, c the concentration of substrate, and I_{max} the maximum current measured under the saturated substrate condition. The K_M^{app} value for the RGO–PbTe–Hb modified electrode is determined to be 3.23 μM, which is much lower than that of 1.9 mM for Hb in the SP Sephadex membrane on the pyrolytic graphite disk electrode [39], 0.898 mM for Hb immobilized on a carbon paste electrode by a silica sol–gel film [40], 2.87 mM for Hb encapsulated in mesoporous silicas [41], 71.49 μM for Hb intercalated into AuNPs-C@SiO_2 [42], and 0.31 mM for Hb immobilized on zirconium dioxide nanoparticles [43].

The amperometric response of the biosensor was also investigated. The reduction current responsed to the addition of H_2O_2 quickly reached a steady value within 5 s at an applied potential of −0.4 V. The results showed a rapid response time, but poor linear relationship was observed in the range from 0.5 to 30 μM.

The RGO–PbTe nanocomposites not only possess the advantages of graphene [12], such as no toxic, good thermal stability, conductivity and biocompatibility, but also the adsorption affinity of PbTe for the incorporation of Hb into RGO–PbTe, resulting in the increased electron transfer rate between Hb and electrode to produce higher enzymatic activity to H_2O_2 reduction. In addition, the graphene would stabilize and disperse the PbTe nanoparticles through its two-dimensional structure to prevent aggregation. Additional experiments were carried out to test the stability. The electrode was stored in phosphate buffer solution at pH 7.0 in the refrigerator at 4 °C for two weeks and no obvious change was observed. The biosensor retained 96% of its original response after a month when it was investigated by CVs in the presence of 50 μM H_2O_2.

4. Conclusions

In this paper, RGO–PbTe composite was synthesized by sono-electrochemical technique. Due to the high electro-conductivity and good biocompatibility, it was successfully used as a novel component for the fabrication of electrochemical biosensor, which facilitated the direct electron transfer from the biomolecules to the electrode surface. The CV measurements indicated that the reduction current increased with the concentration of H_2O_2. Based on the enhanced electrocatalytic CV response, a H_2O_2 sensor has been developed, which exhibited good linearity in the concentration ranges of from 0.5 to 30 μM with a detection limit of 0.13 μM (S/N = 3). The apparent Michaelis–Menten constant K_M^{app} was estimated to be 3.23 μM that illustrated the excellent biological activity of the immobilized Hb. In addition, the biosensor displayed high sensitivity, good reproducibility and long-term stability.

Acknowledgements

We greatly appreciate the support of the National Natural Science Foundation of China (50972058). This work is also supported by National Basic Research Program of China (2011CB933502). JJS also thanks the support of the National Natural Science Foundation

of China (21071004) and Anhui Provincial Natural Science Foundation (1208085MB27).

Appendix A. Supplementary data

Supplementary data associated with this article can be found, in the online version, at http://dx.doi.org/10.1016/j.snb.2012.06.091.

References

[1] M. Pumera, S. Sanchez, I. Ichinose, J. Tang, Electrochemical nanobiosensors, Sensors and Actuators B 123 (2007) 1195–1205.
[2] D. Li, R.B. Kaner, Graphene-based materials, Science 320 (2008) 1170–1171.
[3] P. Avouris, Graphene: electronic and photonic properties and devices, Nano Letters 10 (2010) 4285–4294.
[4] K.J. Huang, D.J. Niu, X. Liu, Z.W. Wu, Y. Fan, Y.F. Chang, Y.Y. Wu, Direct electrochemistry of catalase at amine-functionalized graphene/gold nanoparticles composite film for hydrogen peroxide sensor, Electrochimica Acta 56 (2011) 2947–2953.
[5] Y. Zhou, S. Liu, H.J. Jiang, H. Yang, H.Y. Chen, Direct electrochemistry and bioelectrocatalysis of microperoxidase-11 immobilized on chitosan–graphene nanocomposite, Electroanalysis 22 (2010) 1323–1328.
[6] J.F. Wu, M.Q. Xu, G.C. Zhao, Graphene-based modified electrode for the direct electron transfer of cytochrome *c* and biosensing, Electrochemistry Communications 12 (2010) 175–177.
[7] K. Wang, Q. Liu, Q.M. Guan, J. Wu, H.N. Li, J.J. Yan, Enhanced direct electrochemistry of glucose oxidase and biosensing for glucose via synergy effect of graphene and CdS nanocrystals, Biosensors and Bioelectronics 26 (2011) 2252–2257.
[8] C.S. Shan, H.F. Yang, J.F. Song, D.X. Han, A. Ivaska, L. Niu, Direct electrochemistry of glucose oxidase and biosensing for glucose based on graphene, Analytical Chemistry 81 (2009) 2378–2382.
[9] Q. Zhang, Y. Qiao, F. Hao, L. Zhang, S.Y. Wu, Y. Li, J.H. Li, X.M. Song, Fabrication of a biocompatible and conductive platform based on a single-stranded DNA/graphene nanocomposite for direct electrochemistry and electrocatalysis, Chemistry: A European Journal 16 (2010) 8133–8139.
[10] M.G. Li, S.D. Xu, M. Tang, L. Liu, F. Gao, Y.L. Wang, Direct electrochemistry of horseradish peroxidase on graphene-modified electrode for electrocatalytic reduction towards H_2O_2, Electrochimica Acta 56 (2011) 1144–1149.
[11] H.L. Guo, D.Y. Liu, X.D. Yu, X.H. Xia, Direct electrochemistry and electrocatalysis of hemoglobin on nanostructured gold colloid-silk fibroin modified glassy carbon electrode, Sensors and Actuators B 139 (2009) 598–603.
[12] R. Muszynski, B. Seger, P. Kamat, Decorating graphene sheets with gold nanoparticles, Journal of Physical Chemistry C 112 (2008) 5263–5266.
[13] W.J. Hong, H. Bai, Y.X. Xu, Z.Y. Yao, Z.Z. Gu, G.Q. Shi, Preparation of gold nanoparticle/graphene composites with controlled weight contents and their application in biosensors, Journal of Physical Chemistry C 114 (2010) 1822–1826.
[14] G. Williams, B. Seger, P.V. Kamat, TiO_2–graphene nanocomposites. UV-assisted photocatalytic reduction of graphene oxide, ACS Nano 7 (2008) 1487–1491.
[15] K.S. Kim, Y. Zhao, H. Jang, S.Y. Lee, J.M. Kim, K.S. Kim, J.H. Ahn, P. Kim, J.Y. Choi, B.H. Hong, Large-scale pattern growth of graphene films for stretchable transparent electrodes, Nature 457 (2009) 706–710.
[16] X.Y. Zhang, H.P. Li, X.L. Cui, Y.H. Lin, Graphene/TiO_2 nanocomposites: synthesis, characterization and application in hydrogen evolution from water photocatalytic splitting, Journal of Materials Chemistry 20 (2010) 2801–2806.
[17] J.J. Shi, J.J. Zhu, Sonoelectrochemical fabrication of Pd–graphene nanocomposite and its application in the determination of chlorophenols, Electrochimica Acta 56 (2011) 6008–6013.
[18] J.J. Shi, G.H. Yang, J.J. Zhu, Sonoelectrochemical fabrication of PDDA–RGO–PdPt nanocomposites as electrocatalyst for DAFCs, Journal of Materials Chemistry 21 (2011) 7343–7349.
[19] T. Kuila, S. Bose, P. Khanra, A.K. Mishra, N.H. Kim, J.H. Lee, Recent advances in graphene-based biosensors, Biosensors and Bioelectronics 26 (2011) 4637–4648.
[20] F.W. Wise, Lead salt quantum dots: the limit of strong quantum confinement, Accounts of Chemical Research 33 (2000) 773–780.
[21] Z.W. Quan, L. Valentin-Bromberg, W.S. Loc, J.Y. Fang, Self-assembly of lead chalcogenide nanocrystals, Chemistry: An Asian Journal 6 (2011) 1126–1136.
[22] S.A. McDonald, G. Konstantatos, S. Zhang, P.W. Cyr, E.J.D. Klem, L. Levina, E.H. Sargent, Solution-processed PbS quantum dot infrared photodetectors and photovoltaics, Nature Materials 4 (2005) 138–142.
[23] J.B. Gao, J.M. Luther, O.E. Semonin, R.J. Ellingson, A.J. Nozik, M.C. Beard, Quantum dot size dependent *J–V* characteristics in heterojunction ZnO/PbS quantum dot solar cells, Nano Letters 11 (2011) 1002–1008.
[24] M.G. Kanatzidis, Nanostructured thermoelectrics: the new paradigm? Chemistry of Materials 22 (2010) 648–659.
[25] L. Etgar, E. Lifshitz, R. Tannenbaum, Hierarchical conjugate structure of gamma-Fe_2O_3 nanoparticles and PbSe quantum dots for biological applications, Journal of Physical Chemistry C 111 (2007) 6238–6244.
[26] Y.Y. Wang, K.F. Cai, J.L. Yin, B.J. An, Y. Du, X. Yao, In situ fabrication and thermoelectric properties of PbTe–polyaniline composite nanostructures, Journal of Nanoparticle Research 13 (2011) 533–539.
[27] Y.Y. Wang, K.F. Cai, X. Yao, Facile fabrication and thermoelectric properties of PbTe-modified poly (3,4-ethylenedioxythiophene) nanotubes, ACS Applied Materials & Interfaces 3 (2011) 1163–1166.
[28] C. Erk, A. Berger, J.H. Wendorff, S. Schlecht, Polymer-assisted preparation of nanoscale films of thermoelectric PbSe and PbTe and of lead chalcogenide–polymer composite films, Dalton Transactions 39 (2010) 11248–11254.
[29] G. Eda, M. Chhowalla, Graphene-based composite thin films for electronics, Nano Letters 9 (2009) 814–818.
[30] A. Gedanken, Using sonochemistry for the fabrication of nanomaterials, Ultrasonics Sonochemistry 11 (2004) 47–55.
[31] V. Sáez, T.J. Mason, Sonoelectrochemical synthesis of nanoparticles, Molecules 14 (2009) 4284–4299.
[32] J.H. Bang, K.S. Suslick, Applications of ultrasound to the synthesis of nanostructured materials, Advanced Materials 22 (2010) 1039–1059.
[33] Q.M. Shen, Q.H. Min, J.J. Shi, L.P. Jiang, J.R. Zhang, W.H. Hou, J.J. Zhu, Morphology-controlled synthesis of palladium nanostructures by sonoelectrochemical method and their application in direct alcohol oxidation, Journal of Physical Chemistry C 113 (2009) 1267–1273.
[34] W.S. Hummers, R.E. Offeman, Preparation of graphitic oxide, Journal of the American Chemical Society 6 (1958) 1339–1340.
[35] X.F. Qiu, Y.B. Lou, A.C.S. Samia, A. Devadoss, J.D. Burgess, S. Dayal, C. Burda, PbTe nanorods by sonoelectrochemistry, Angewandte Chemie International Edition 44 (2005) 5855–5857.
[36] J.J. Zhang, Y.G. Liu, L.P. Jiang, J.J. Zhu, Synthesis, characterizations of silica-coated gold nanorods and its applications in electroanalysis of hemoglobin, Electrochemistry Communications 10 (2008) 355–358.
[37] W. Sun, D.D. Wang, R.F. Gao, K. Jiao, Direct electrochemistry and electrocatalysis of hemoglobin in sodium alginate film on a $BMIMPF_6$ modified carbon paste electrode, Electrochemistry Communications 9 (2007) 1159–1164.
[38] R.A. Kamin, G.S. Wilson, Rotating ring-disk enzyme electrode for biocatalysis kinetic studies and characterization of the immobilized enzyme layer, Analytical Chemistry 52 (1980) 1198–1250.
[39] C.H. Fan, H.Y. Wang, S. Sun, D.X. Zhu, F. Wagner, G.X. Li, Electron-transfer reactivity and enzymatic activity of hemoglobin in a SP sephadex membrane, Analytical Chemistry 73 (2001) 2850–2854.
[40] Q.L. Wang, G.X. Lu, B.J. Yang, Hydrogen peroxide biosensor based on direct electrochemistry of hemoglobin immobilized on carbon paste electrode by a silica sol–gel film, Sensors and Actuators B 99 (2004) 50–57.
[41] Y.Z. Xian, Y. Xian, L.H. Zhou, F.H. Wu, Y. Ling, L.T. Jin, Encapsulation hemoglobin in ordered mesoporous silicas: influence factors for immobilization and bioelectrochemistry, Electrochemistry Communications 9 (2007) 142–148.
[42] Y.Y. Wang, X.J. Chen, J.J. Zhu, Fabrication of a novel hydrogen peroxide biosensor based on the AuNPs-C@ SiO_2 composite, Electrochemistry Communications 11 (2009) 323–326.
[43] S.Q. Liu, Z.H. Dai, H.Y. Chen, H.X. Ju, Immobilization of hemoglobin on zirconium dioxide nanoparticles for preparation of a novel hydrogen peroxide biosensor, Biosensors and Bioelectronics 19 (2004) 963–969.

Biographies

Jian-Jun Shi is an associate professor of applied chemistry at School of Chemical Engineering, Anhui University of Science and Technology, earned PhD degree at Nanjing University in 2011. His research focuses on sonoelectrochemistry and biosensor.

Wei Hu is a M.S. student at School of Chemical Engineering, Anhui University of Science and Technology. He worked at Nanjing University as a visiting student in 2011.

Dan Zhao is a M.S. student at School of Chemistry and Chemical Engineering, Nanjing University.

Ting-Ting He is a M.S. student at School of Chemical Engineering, Anhui University of Science and Technology.

Jun-Jie Zhu is a professor of analytical chemistry at School of Chemistry and Chemical Engineering, Nanjing University. His research focuses on preparation and characterization of nanomaterials, bioelectrochemistry and nanoelectrochemistry.